

# Probing for Leptonic Signatures from GRB030329 with AMANDA-II



**Michael Stamatikos**

**University of Wisconsin, Madison**

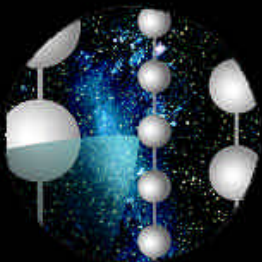
**Department of Physics**

**[michael.stamatikos@icecube.wisc.edu](mailto:michael.stamatikos@icecube.wisc.edu)**

**TeV Particle Astrophysics Workshop 2005**

**Fermi National Laboratory, Batavia IL**

**July 14, 2005**



**IceCube**



# **Talk Overview**

## **I. Introduction & Motivation:**

- A. GRBs: Electromagnetic observables.
- B. Fireball phenomenology & the GRB-neutrino connection.
- C. GRB030329: a case study.

## **II. Neutrino Astronomy & AMANDA-II:**

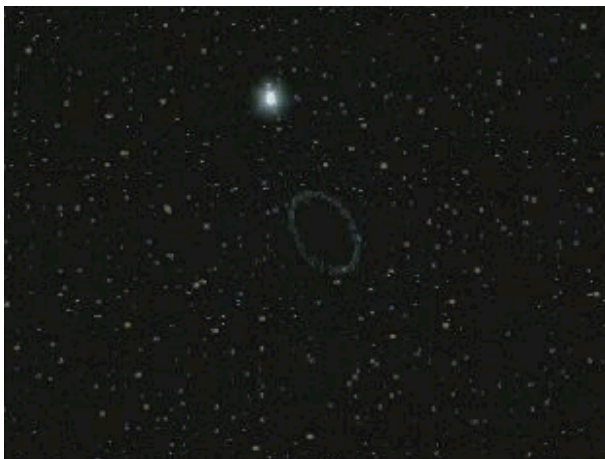
- A. Flux models and detector response.
- B. Optimization methods.

## **III. Results:**

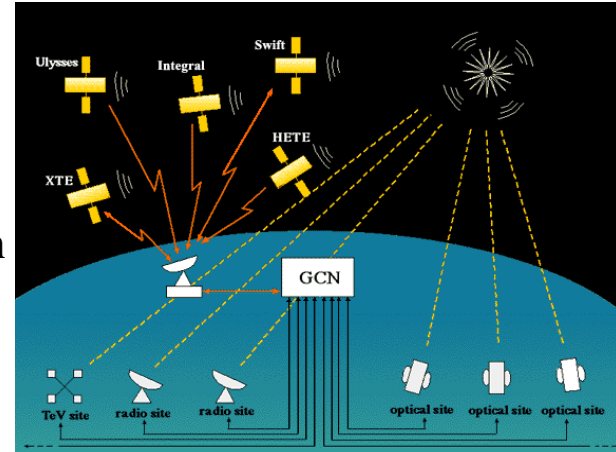
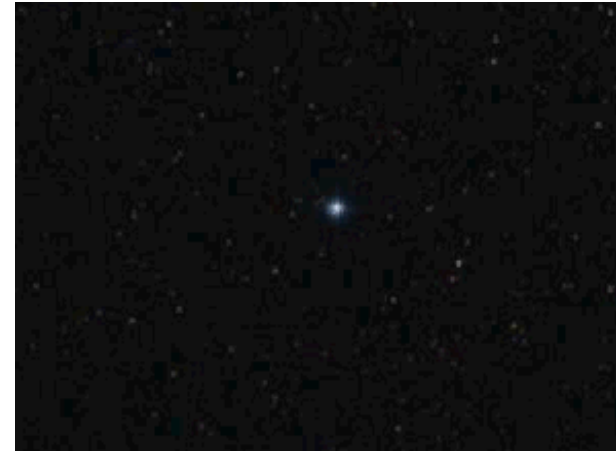
- A. Neutrino flux upper limits for various models.
- B. Comparison with other authors.

## **IV. Conclusions & Future Outlook:**

- A. Implications for correlative leptonic-GRB searches.



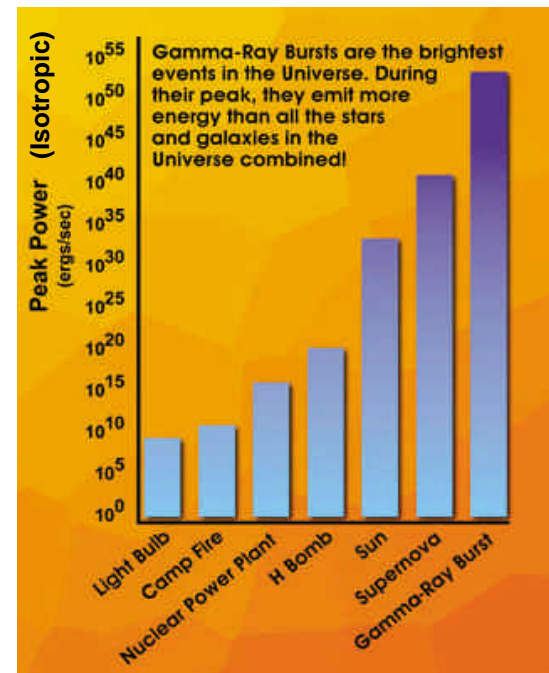
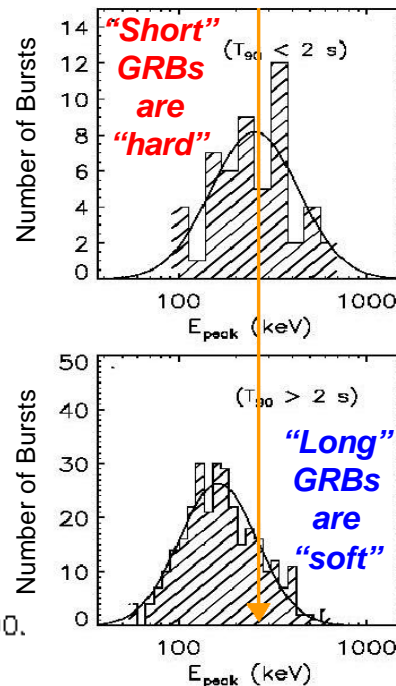
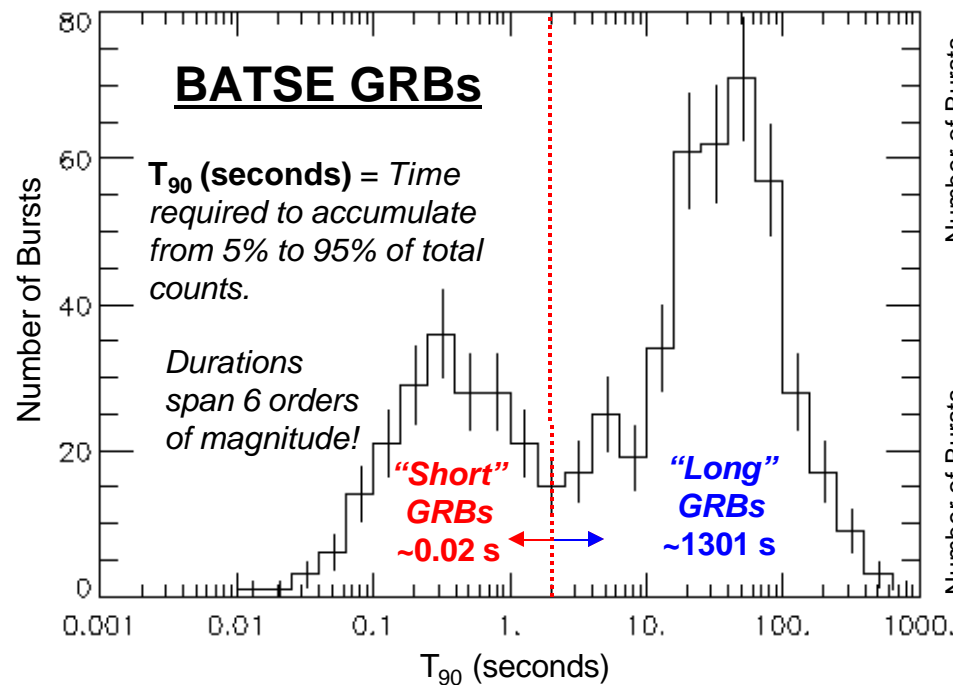
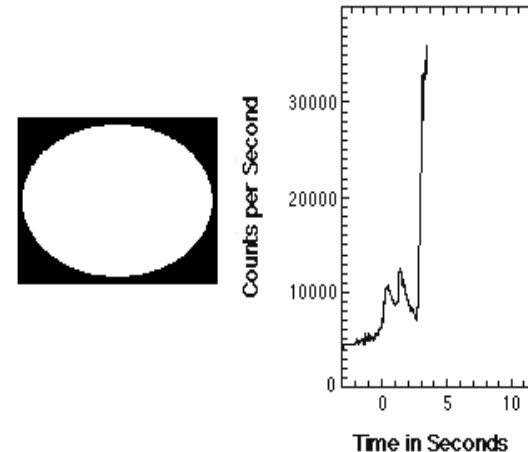
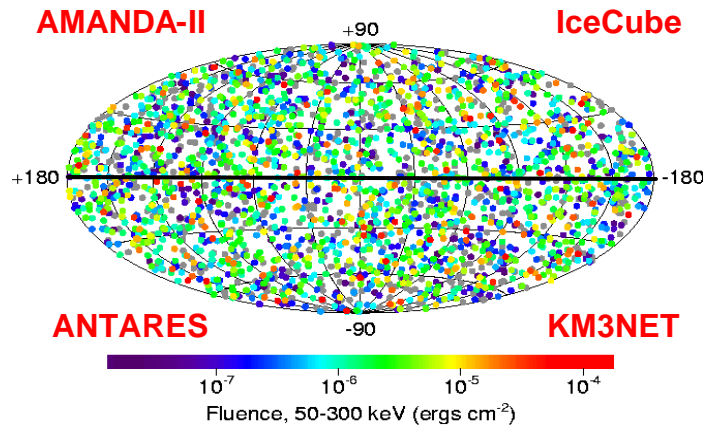
- Gamma-ray bursts (GRBs), discovered in the early 1970's by Vela satellites, are isotropically distributed transients of  $\sim \text{keV} - \sim 20 \text{ GeV}$  radiation lasting for  $\sim 0.01 - \sim 1000$  seconds.
- The Burst and Transient Source Experiment (BATSE) triggered over 2700 GRBs from 1993-2000, averaging about 1 GRB/day @  $\sim 2/3$  sky coverage.
- Progenitor models include compact binary mergers and the collapse of massive stars.
- The standard model of GRBs is characterized by the fireball phenomenology.
- GRB030329, detected by HETE-II, was a watershed transient, clinching the connection between GRBs and Type Ic SN. Due to rapid response via the GRB Coordinate Network (GCN).



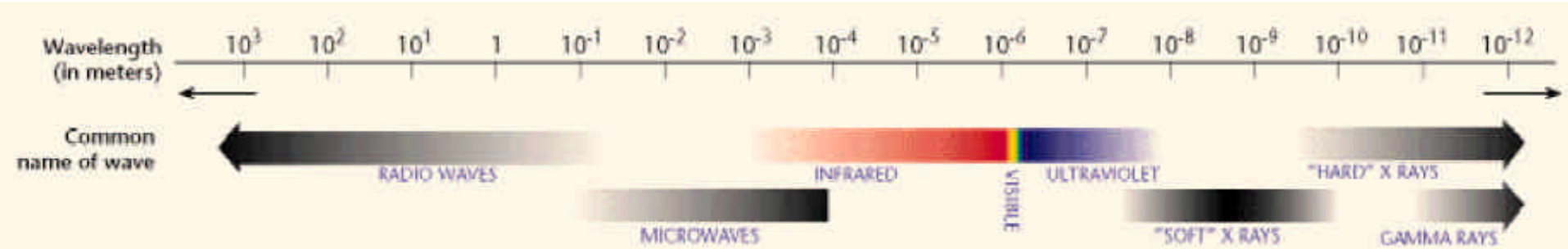


# Gamma-Ray Bursts (GRBs): Prompt Emission

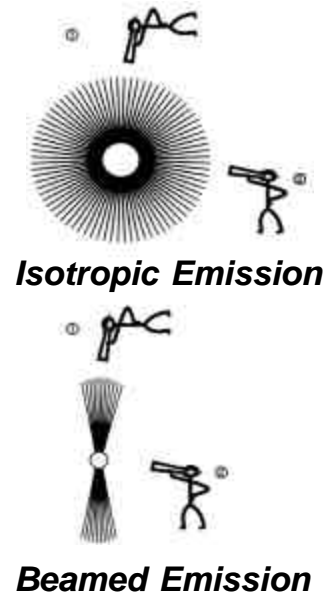
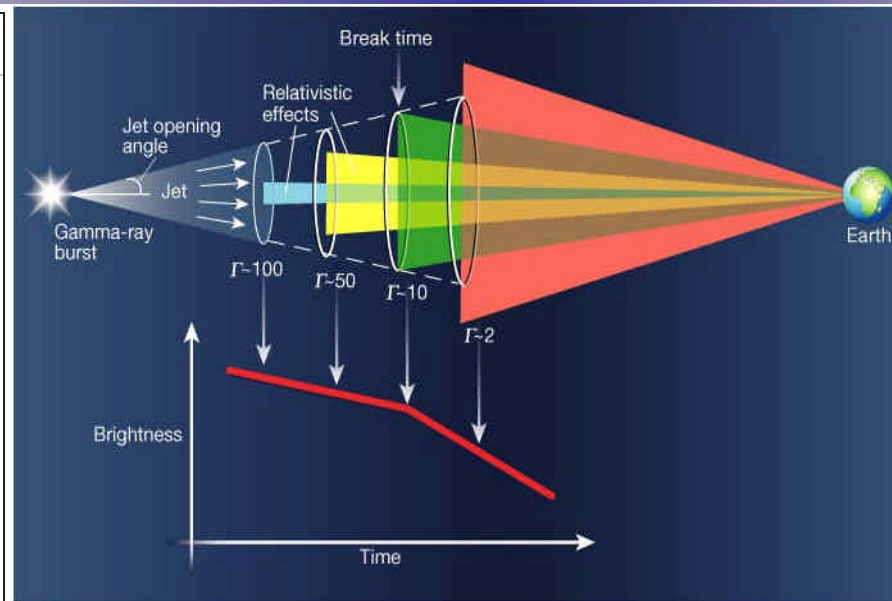
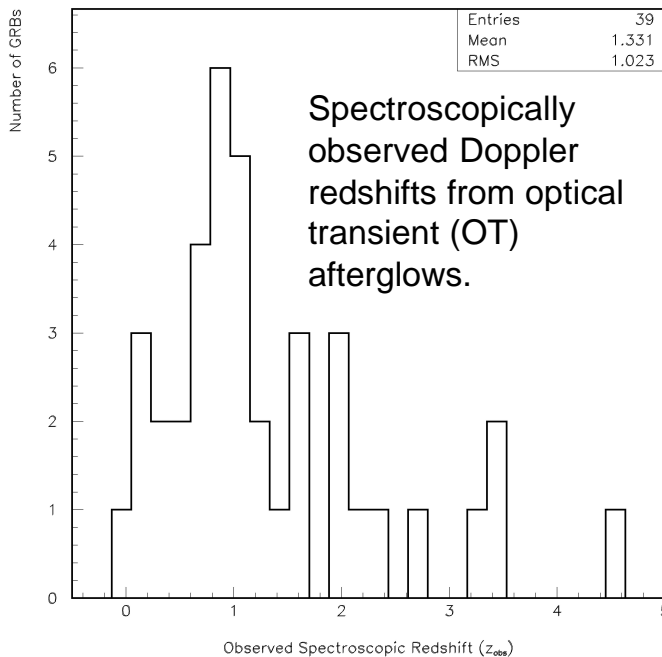
- GRBs are unique, varying from burst to burst and class to class (short, long, X-ray rich, non-triggered).
- Super-Eddington luminosities imply relativistic expansion.
- Millisecond temporal variability implies compact objects  $R = 2\Gamma^2 c \Delta t$ .
- Compactness problem resolved via  $\sim 100 = \Gamma_{\text{Bulk}} = \sim 1000$ , ensuring transparent optical depth to observed  $\gamma$ -ray photons, i.e.  $\tau_{\gamma\gamma} = 1$ .



# GRBs: Multi-Wavelength EM Afterglows



## Prompt Afterglow



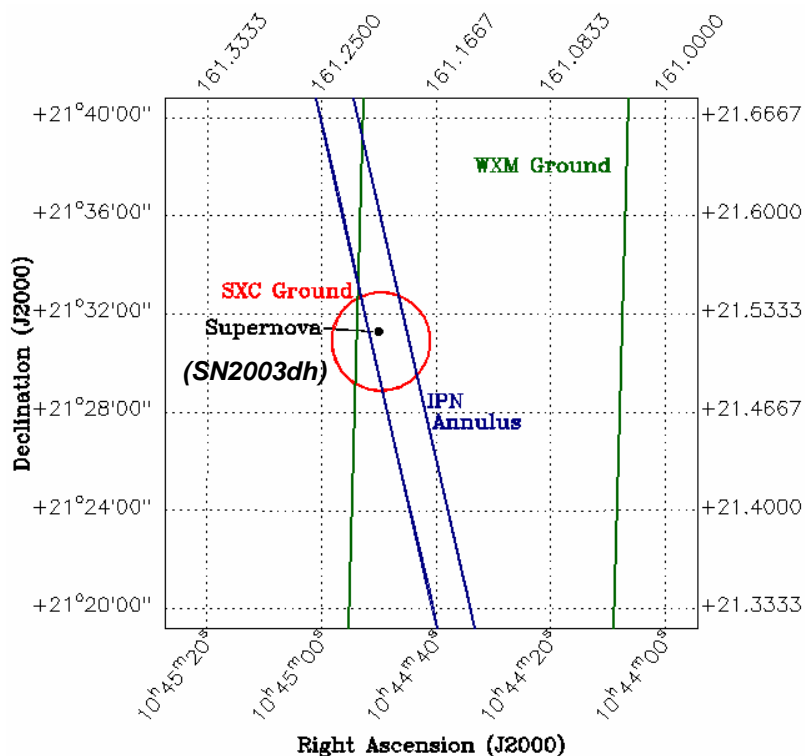
**Isotropic Emission:**  $\sim 1$  GRB/Day  $\rightarrow R_{\text{GRB}}^{\text{iso}} \sim 0.5$  GRB/(Gpc<sup>3</sup>·yr).

**Beamed (Jet) Emission:** Corrections  $\rightarrow R_{\text{GRB}}^{\text{iso}} \cdot (4\pi/\Omega_b)$  sr and  $E_{\gamma}^{\text{iso}} \cdot (\Omega_b/4\pi)$  sr. Where:  $\Omega_b$  = Beaming solid angle (sr).

$$f_b \equiv 1 - \cos \theta_{\text{jet}} \equiv \text{Beaming fraction}$$

$$\theta_{\text{jet}} \approx 1/\Gamma_{\text{Bulk}} \quad \Gamma_{\text{Bulk}} = \frac{1}{\sqrt{1 - v^2/c^2}}$$

# GRB030329: Initial Localization & Temporal Spectrum



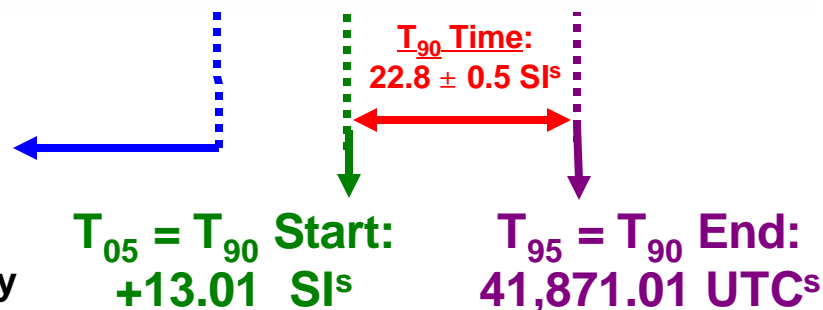
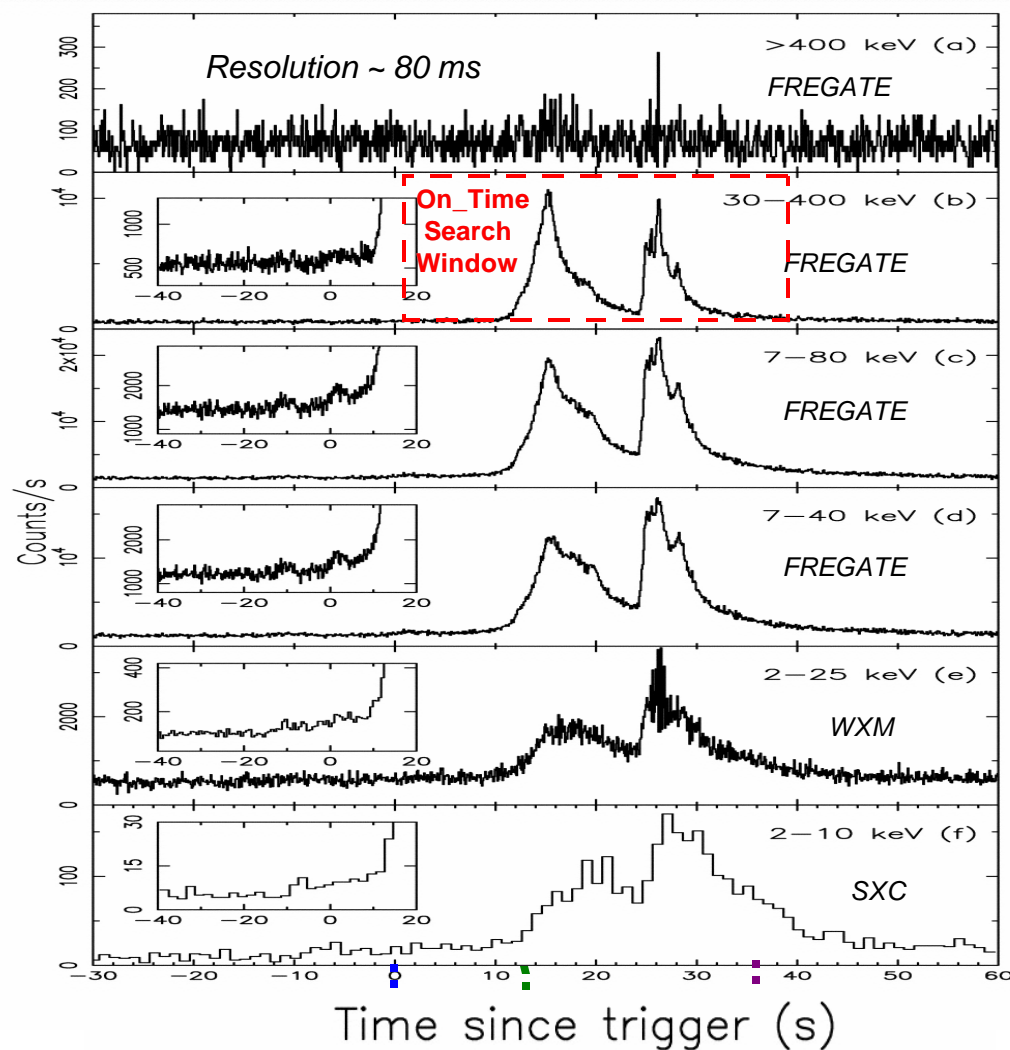
Wide-Field X-ray Monitor (WXM):  
2-25 keV, accurate to  $\approx 10^\circ$ .

Soft X-ray Camera (SXC):  
0.5-10 keV, accurate to  $\approx 0.5^\circ$ .

French Gamma Telescope (FREGATE):  
6-400 keV,  $70^\circ$  FOV

**Trigger Time:**  
**41,834.7 UTC<sup>s</sup>**

**30-400 keV Energy  
Band Pass**



*Vanderspek, R. et al. ApJ 617, 1251-1257 (2004)*

# GRB030329: Band Photon Energy Spectrum

- Although the temporal spectra are unique, the energy spectra may be fit an empirical *Band function*, provided the parameters are allowed to vary.

$$N_{e_g}(e_g) = \begin{cases} A_g \left( \frac{e_g}{100 \text{ keV}} \right)^a e^{\left( \frac{e_g}{e_g^o} \right)} & (a-b)e_g^o \geq e_g \\ A_g \left[ \frac{(a-b)e_g^o}{100 \text{ keV}} \right]^{(a-b)} e^{(b-a)} \left( \frac{e_g}{100 \text{ keV}} \right)^b & (a-b)e_g^o \leq e_g \end{cases}$$

*Band, D.L. et al. ApJ 413, 281-292 (1993)*

Prompt gamma - ray emission :

$$\text{Fluence } (F_g) = 1.630_{-0.013}^{+0.014} \times 10^{-4} \frac{\text{ergs}}{\text{cm}^2}$$

*Sakamoto, T. et al. astro-ph/0409128*

$$\text{Peak Flux } (\Phi_g^{\text{Peak}}) \sim 7 \times 10^{-6} \frac{\text{ergs}}{\text{cm}^2 \cdot \text{s}}$$

*Vanderspek, R. et al. GCN Report 2212*

Band Spectral Fit Parameters :

$$a = -1.32 \pm 0.02 > -2 \equiv \text{Low Index}$$

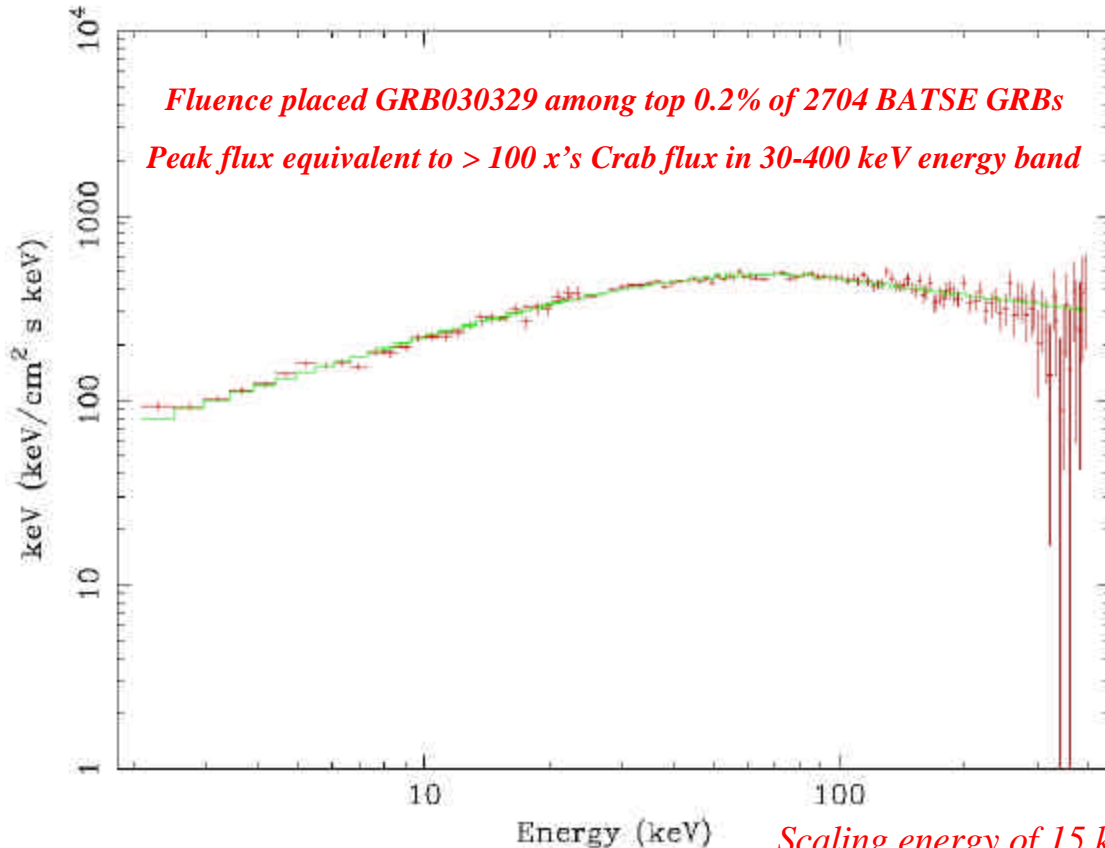
$$b = -2.44 \pm 0.08 < -2 \equiv \text{High Index}$$

$$e_g^P = 70.2 \pm 2.3 \text{ keV} \equiv \text{Peak Energy}$$

*Vanderspek, R. et al. ApJ 617, 1251-1257 (2004)*

$$e_g^o = e_g^P / (2 + a) = 103.2 \pm 4.5 \text{ keV}$$

$$\text{Photon break energy} = e_g^b = (a - b)e_g^o = 115.6 \pm 9.9 \text{ keV}$$

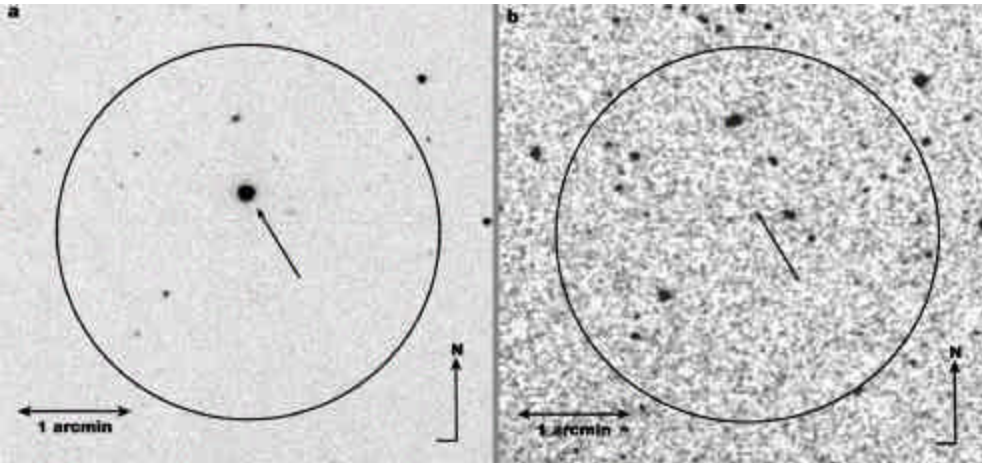


*Barraud, C. et al. astro-ph/0311630*



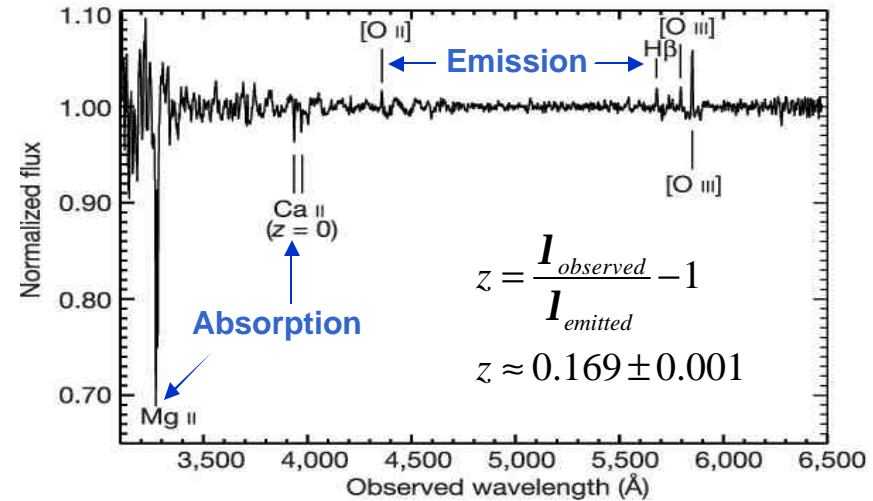
# GRB03029: Optical Transient (OT) Afterglow

HETE-II SXC 4' error circle is shown in both plates.



600<sup>s</sup> exposure taken on 13<sup>h</sup>5<sup>m</sup> UTC, 29 March 2003 (~1.5<sup>h</sup> after prompt γ-ray emission).

Comparison with Second Digitized Sky Survey (DSS2) identified 12 magnitude OT.



Low Resolution Imaging Spectrometer on Keck I (600<sup>s</sup> @ 4.2 Å)

Price, P.A. et al., *Nature* 423, 844-847 (2003)

$$L_g^{\text{iso}} = \Phi_g^{\text{Peak}} 4\pi d_L^2, \Phi_g^{\text{Peak}} \approx 7 \times 10^{-6} \frac{\text{ergs}}{\text{cm}^2 \cdot \text{s}} \& z = 0.168541 \pm 0.000004$$

Bloom, J. et al. GCN Report 2212

$$d_L = \frac{c(1+z)}{H_o} \int_0^z \frac{dz'}{\sqrt{\Omega_\Lambda + \Omega_m(1+z')^3}}, \Lambda_{CDM} \Rightarrow \left\{ \begin{array}{l} H_o = 72 \pm 5 \frac{\text{km}}{\text{s} \cdot \text{Mpc}} \\ \Omega_M = 0.29 \pm 0.07 \\ \Omega_\Lambda = 0.73 \pm 0.09 \\ z = 0.168541 \pm 0.000004 \end{array} \right\}$$

Spergel et al., *ApJS* 148, 175-194 (2003)

**Redshift + Assumed Cosmological Model<sup>®</sup> Luminosity distance, which sets the energy scale**

$$d_L \approx 2.44^{+0.20}_{-0.18} \times 10^{27} \text{ cm}$$

$$L_g^{\text{iso}} \approx 5.24^{+0.86}_{-0.77} \times 10^{50} \frac{\text{ergs}}{\text{s}} \quad [30 - 400 \text{ keV band pass}]$$

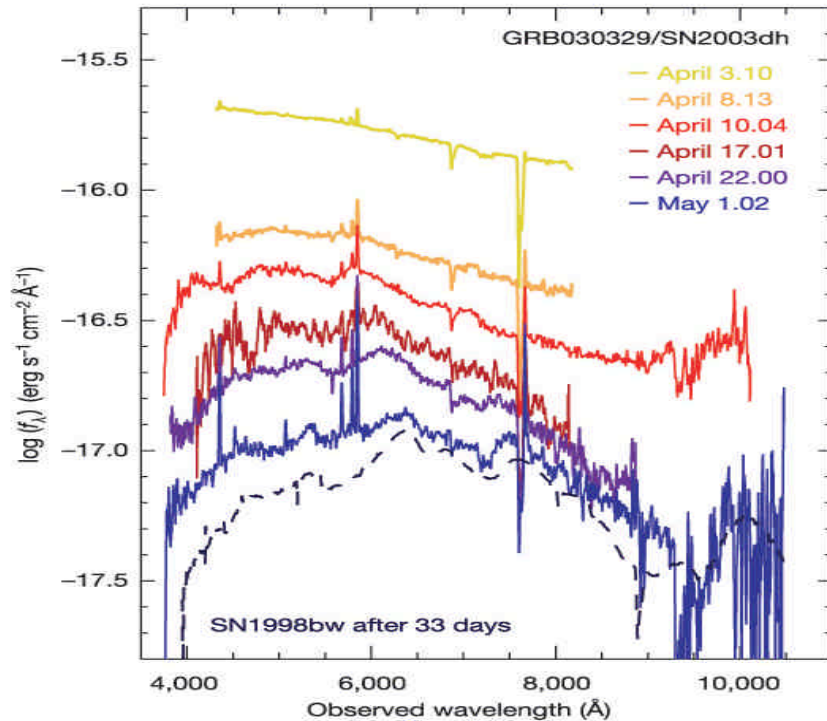
Close but Under-luminous

Close by GRB standards but still cosmological;  $d_L \sim 2.2$  billion light years → Corresponds to Precambrian geologic time, i.e. predates the Earth's first ice age, when Antarctica was located in northern hemisphere!

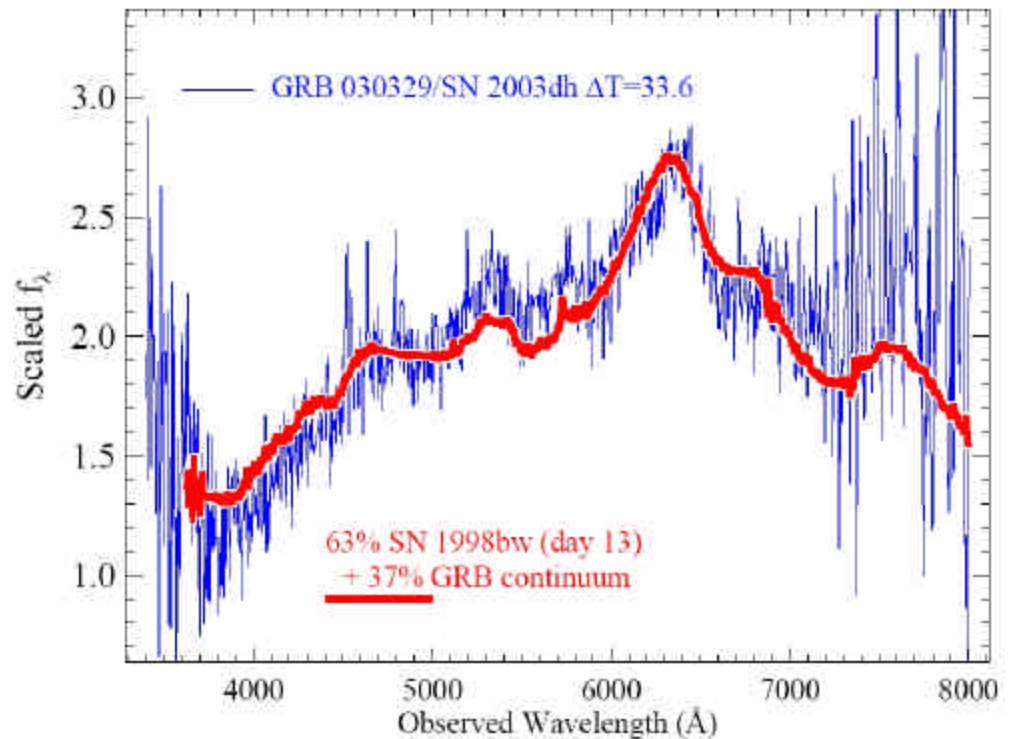


# OT Spectral Evolution: GRB2003/SN2003dh

- GRBs/Type Ic SN connection → Collapsar progenitor model.
- Observations consistent with fireball description. Exposed problems with the Cannon Ball model [Dado et al., ApJ 594, L89-L92 (2003)]; as discussed in Taylor et al., ApJ 609 L1-L4 (2004) and Oren et al., MNRAS 353, L35-L40 (2004).

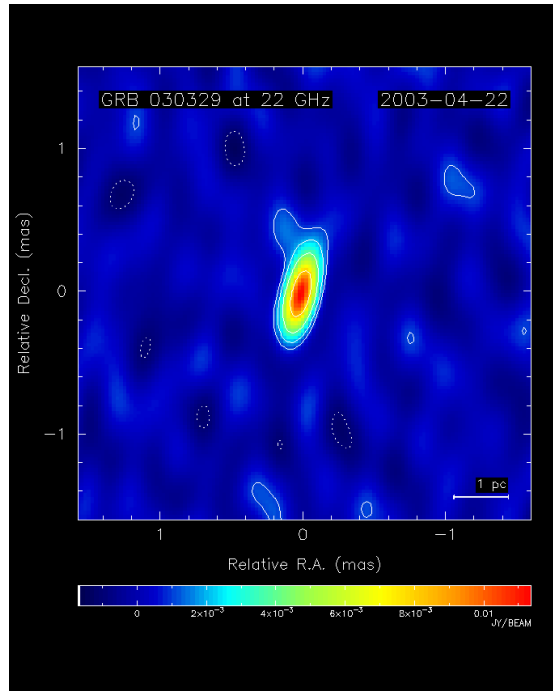


Hjorth et al., Nature 423, 847-850 (2003)



Matheson et al., astro-ph/0307435

# GRB030329 Radio Afterglow



- Radio Counterpart of GRB030329, leads to *mas* positional localization.

$$\mathbf{a}_{J\,2000} = 10^h 44^m 49.^s 9595$$

$$= 161.2081646^\circ$$

$$\mathbf{d}_{J\,2000} = +21^\circ 31' 17.'' 438$$

$$= 21.5215106^\circ$$

$$\pm \mathbf{s}_R = 0.''001 = (3 \times 10^{-7})^\circ$$

*Taylor et al., GCN Report 2129*

- Radio calorimetry revealed break in the afterglow spectrum consistent with collimated prompt emission within a jet of opening half angle  $\theta_{\text{jet}} \sim 5^\circ \sim 0.09 \text{ rad}$  [Berger et al., *Nature* 426, 154-157 (2003)]. Requires beaming fraction correction:

$$L_g^{\text{jet}} = L_g^{\text{iso}} (1 - \cos \mathbf{q}_{\text{jet}}) = 1.99_{-0.29}^{+0.33} \times 10^{48} \frac{\text{ergs}}{\text{s}}$$

- Radio calorimetry provided estimates for fraction of shock energy imparted to the electrons ( $\epsilon_e \sim 0.19$ ) and magnetic field ( $\epsilon_B \sim 0.042$ ) [Frail et al, *ApJ* 619, 994-998 (2005)].

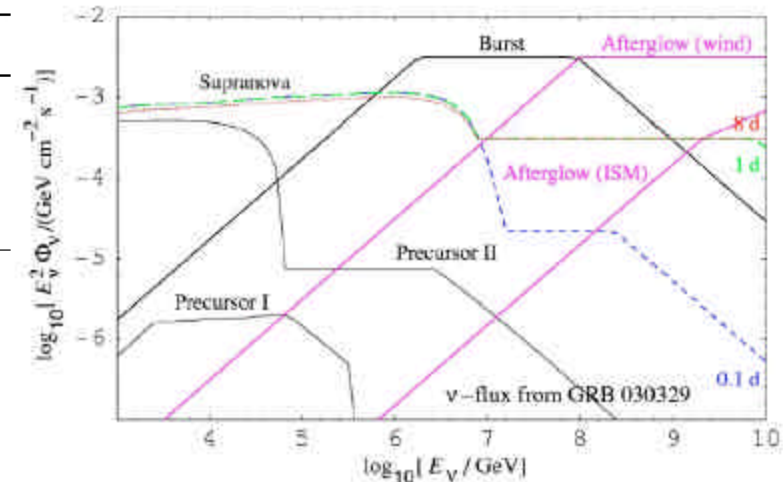
# Leptonic Emission from GRBs?

- Fireball phenomenology predicts MeV-EeV neutrinos in the context of hadronic acceleration.

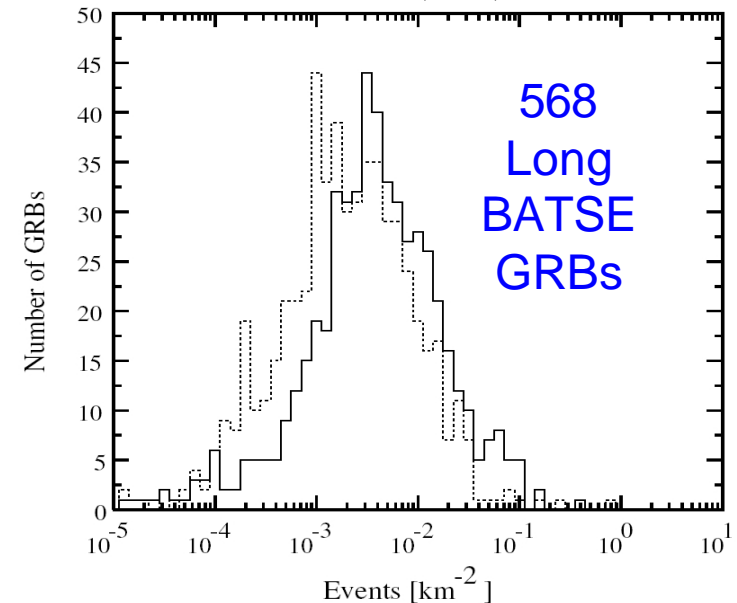
Regime	$\varepsilon_\nu$ (eV)	Mechanism/Comments
1	$\sim 10^7$	Collapse/merger of progenitor event (quasi-thermal)
2	$\sim 10^9 - 10^{10}$	Longitudinal decoupling of the baryonic (i.e. $n, p$ ) flow in fireball
3	$\sim 10^{12} - \leq 10^{14}$	Precursors $\sim 10 - 100$ sec before $\gamma_{\text{Prompt}}$ ( $pp, p\gamma$ between jet/star)
4	$\sim 10^{14} - 10^{15}$	Photomeson interactions/internal shock, simultaneous* with $\gamma_{\text{Prompt}}$
5	$\sim 10^{17} - 10^{18}$	Afterglow, $p\gamma$ /external (reverse) shock, $\sim 10$ seconds after $\gamma_{\text{Prompt}}$

\* Flight time delay due to neutrino mass is negligible for  $\varepsilon_\nu \sim \text{PeV}$ .

- Observationally advantageous are TeV-PeV neutrinos – spatial and temporal coincidence with prompt emission results in nearly background free search.
- Original predictions [Waxman & Bahcall, Phys. Rev. D 59 023002], assumed GRBs were CR accelerators and featured averaged BATSE GRB parameters.
- Electromagnetic observables of GRBs are characterized by distributions which span orders of magnitude and differ from burst to burst and class to class.
- Fluctuations may enhance neutrino production [Halzen & Hooper ApJ 527, L93-L96 (1999), Alvarez-Muniz, Halzen & Hooper Phys. Rev. D 62, (2000)].
- Positive signal detection is a smoking gun signature of hadronic acceleration – may reveal astrophysical source of CR as well as the microphysics associated with GRBs and intrinsic leptonic properties such as neutrino mass.

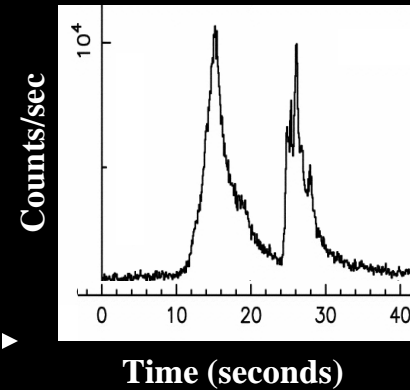
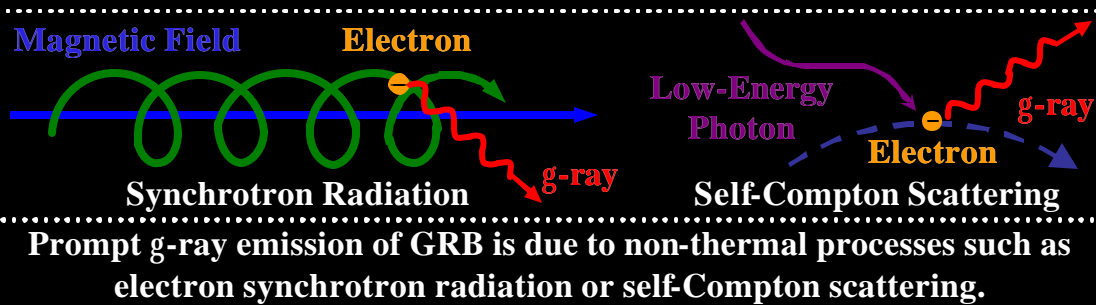


Razzaque, Meszaros & Waxman Phys. Rev. D. 69 023001 (2004)



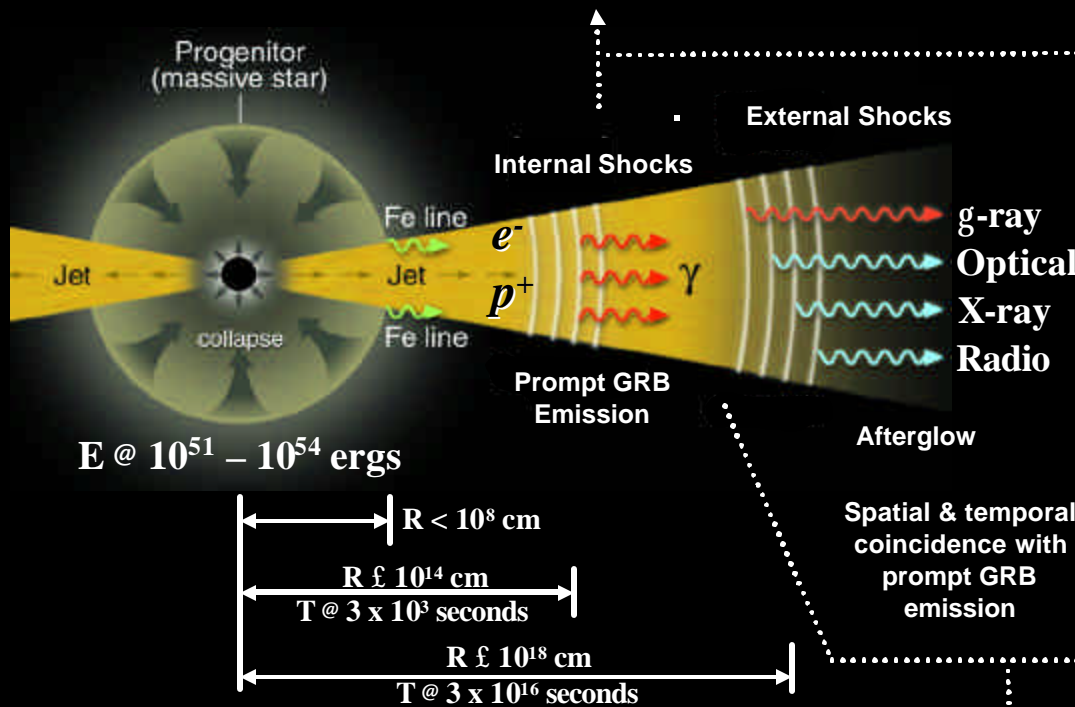
Guetta et al., Astro. Part. 20 (2004) 429-455

# The Fireball Phenomenology: GRB-n Connection

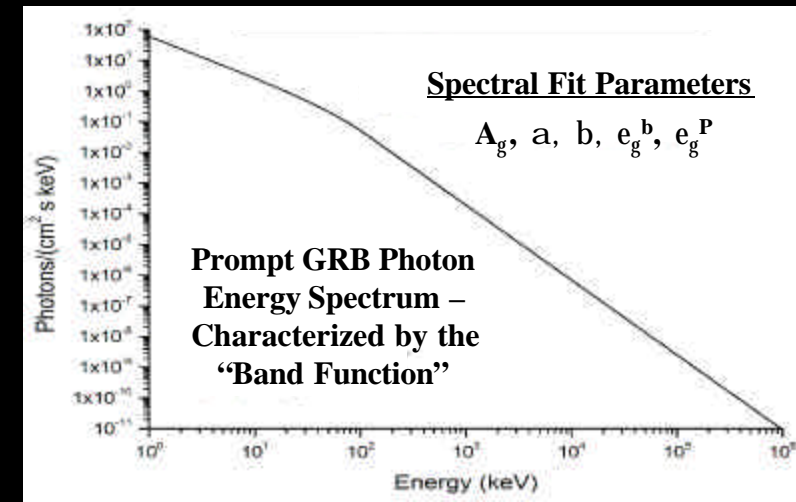
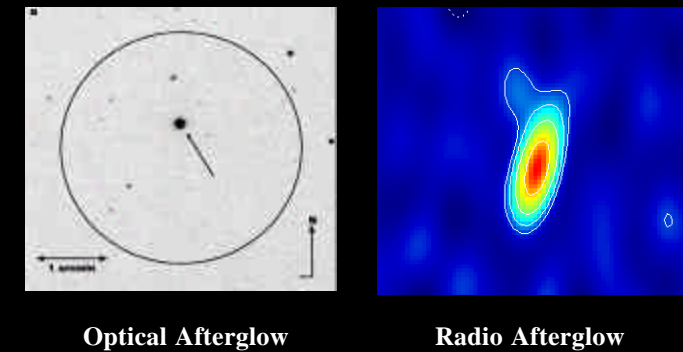


## GRB Prompt Emission (Temporal) Light Curve

- Shock variability is a unique “finger-print” reflected in the complexity of the GRB time profile.
- Implies compact object.



## Multi-wavelength Afterglows Span EM Spectrum



**$E_{GRB}^{PT} \equiv$  py center of mass energy &  $E_{\Delta^+}^{Th} \equiv \Delta^+$  threshold energy.**

**If  $E_{cm}^{pg} > E_{\Delta^+}^{Th} \Rightarrow p^+ + g \rightarrow \Delta^+ \rightarrow (n) + p^+ \rightarrow n_m + m^+ \rightarrow n_m + e^+ + n_e + \bar{n}_m$**

**Photomeson interactions involving relativistically ( $G \gg 300$ ) shock-accelerated protons ( $E_p \approx 10^{16}$  eV) and synchrotron gamma-ray photons ( $E_g \gg 250$  keV) in the fireball wind yield high-energy muonic neutrinos ( $E_n \gg 10^{14} - 10^{15}$  eV).**



# Muon Neutrino Spectrum: Parameterization

$$e_{n_m}^2 \Phi_{n_m} \approx A_{n_m} \times \left\{ \begin{array}{ll} \left( \frac{e_{n_m}}{e_n^b} \right)^{-b-1} & (e_{n_m} < e_n^b) \\ \left( \frac{e_{n_m}}{e_n^b} \right)^{-a-1} & (e_n^b < e_{n_m} < e_p^b) \\ \left( \frac{e_{n_m}}{e_n^b} \right)^{-a-1} \left( \frac{e_{n_m}}{e_p^b} \right)^{-2} & (e_{n_m} > e_p^b) \end{array} \right\}$$

$$A_{n_m} \approx \frac{F_g f_p}{8 \epsilon_e \ln(10) T_{90}} \equiv \text{Normalization}$$

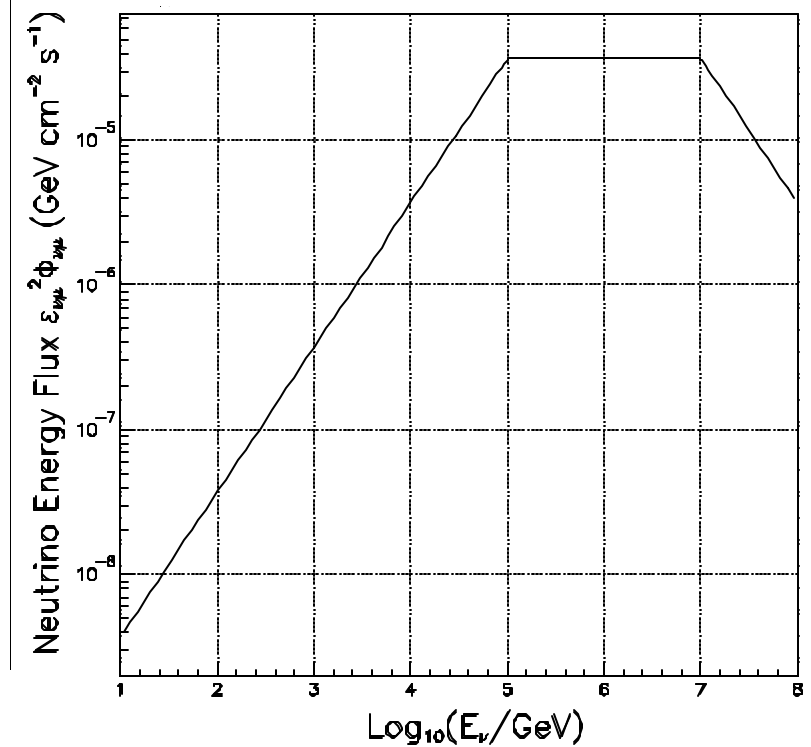
$$f_p \approx 0.2 \times \frac{L_{?,52}}{\Gamma_{2.5}^4 t_{v,-2} e_{?,\text{MeV}}^b (1+z)} \equiv \text{Proton efficiency}$$

$$\Gamma \geq \sim 276 \left[ L_{?,52} t_{v,-2}^{-1} e_{?,\text{MeV}}^{\max} (1+z) \right]^{1/6} \equiv \text{Bulk Lorentz Boost Factor}$$

$$e_n^b \approx \left[ \frac{7 \times 10^5}{(1+z)^2} \frac{\Gamma_{2.5}^2}{e_{?,\text{MeV}}^b} \right] \text{GeV} \equiv \text{Neutrino break energy}$$

$$e_p^b \approx \left[ \frac{10^8}{(1+z)} \epsilon_e^{1/2} \epsilon_B^{-1/2} (L_{?,52})^{-1/2} \Gamma_{2.5}^4 t_{v,-2} \right] \text{GeV} \equiv \text{Synchrotron break energy}$$

Stamatikos, Band, Hooper & Halzen (In preparation)



**Neutrino spectrum is expected to trace the photon spectrum.**

$$e_{n_m} \propto e_p \propto e_g^{-1}$$

$$L_{g,52} \equiv \frac{L_g}{10^{52} \text{ ergs/s}}$$

$$\Gamma_{2.5} \equiv \frac{\Gamma}{10^{2.5}}$$

$$t_{v,-2} \equiv \frac{t_v}{10^{-2} \text{ s}}$$

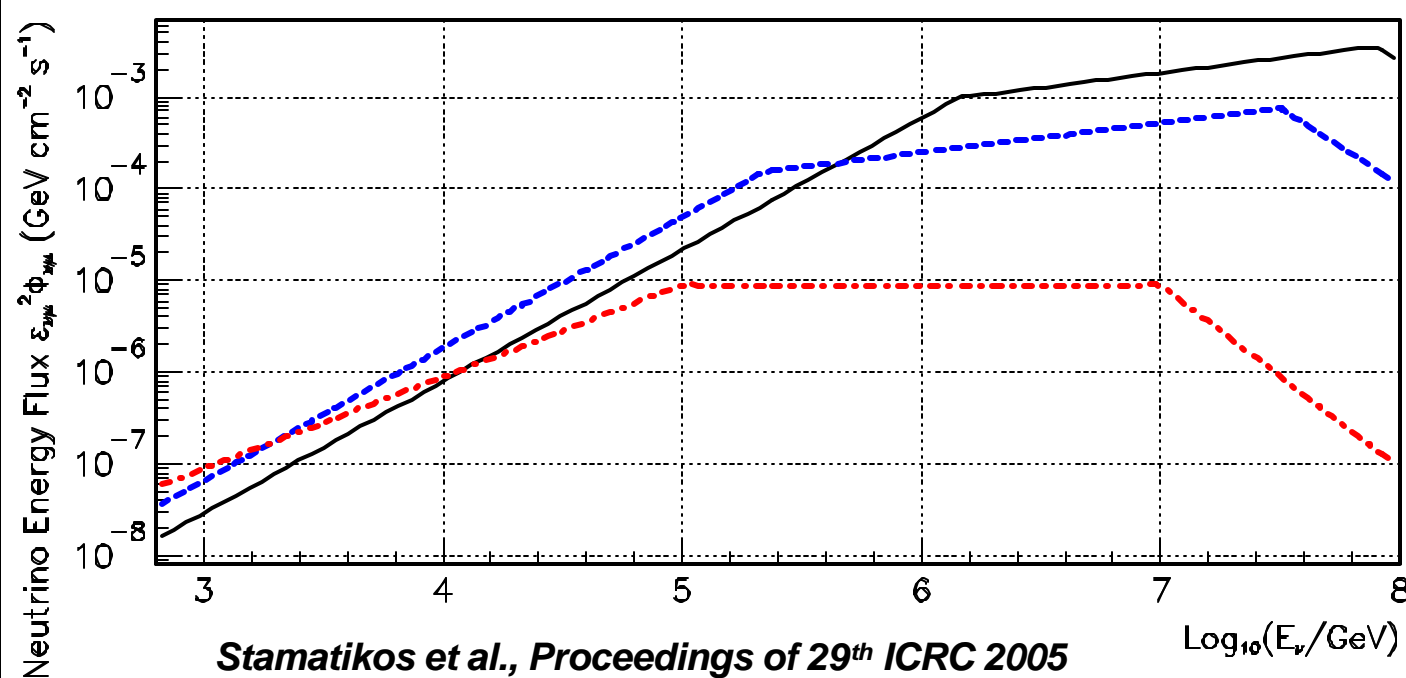
$$e_{?,\text{MeV}}^b \equiv \frac{e_g^b}{1 \text{ MeV}}$$

$$e_{?,\text{MeV}}^{\max} \equiv \frac{e_g}{100 \text{ MeV}}$$

Guetta et al., *Astroparticle Physics* 20, 429-455 (2004)

# Neutrino Flux Models for GRB030329

<u>Model</u>	<u>Model 1</u>	<u>Model 2</u>	<u>Model 3</u>
<u>Parameter</u>	<u>Discrete Isotropic</u>	<u>Discrete Jet</u>	<u>Average Isotropic</u>
Fluence [ $F_\gamma$ ] (ergs/cm <sup>2</sup> )	$(1.63 \pm 0.014) \times 10^{-4}$	$(1.63 \pm 0.014) \times 10^{-4}$	$6.00 \times 10^{-6}$
Peak Flux [ $\Phi_\gamma$ ] (ergs/cm <sup>2</sup> /s)	$\sim 7 \times 10^{-6}$	$\sim 7 \times 10^{-6}$	$2 \times 10^{-6}$
Redshift [z]	$0.168541 \pm 0.000004$	$0.168541 \pm 0.000004$	1
Low Spectral Index [ $\alpha$ ]	$-1.32 \pm 0.02$	$-1.32 \pm 0.02$	-1
High Spectral Index [ $\beta$ ]	$-2.44 \pm 0.08$	$-2.44 \pm 0.08$	-2
Peak Energy [ $\varepsilon_\gamma^p$ ] (keV)	$70.2 \pm 2.3$	$70.2 \pm 2.3$	1000
Break Energy [ $\varepsilon_\gamma^b$ ] (keV)	$115.6 \pm 9.9$	$115.6 \pm 9.9$	1000
Luminosity [ $L_\gamma$ ] (ergs/s)	$(5.24 \pm 0.82) \times 10^{50}$	$(1.99 \pm 0.31) \times 10^{48}$	$1 \times 10^{52}$
Bulk Lorentz Boost [ $\Gamma$ ]	178	70	300
Proton Efficiency [ $f_\pi$ ]	0.77	0.12	0.2
Normalization [ $A_{\nu\mu}$ ] (GeV/cm <sup>2</sup> /s)	$9.86 \times 10^{-4}$	$1.54 \times 10^{-4}$	$8.93 \times 10^{-6}$
Neutrino Break Energy [ $\varepsilon_\nu^b$ ] (GeV)	$1.404951 \times 10^6$	$2.19343 \times 10^5$	$1 \times 10^5$
Synchrotron Break Energy [ $\varepsilon_\pi^b$ ] (GeV)	$7.9832941 \times 10^7$	$3.1543774 \times 10^7$	$1 \times 10^7$



### Neutrino Flux Models

Model 1: Discrete Isotropic

Model 2: Discrete Jet

Model 3: Average Isotropic

$$e_n^b = \left[ \frac{7 \times 10^5}{(1+z)^2} \frac{\Gamma_{2.5}^2}{e_{?,\text{MeV}}^b} \right] \text{GeV}$$

*Up-going Events, Detected via charged current interactions:*

$$n_m + N \rightarrow m^+ + X$$

### IceCube (Dashed)

Model 1: Discrete Isotropic  
(0.1308 events)

Model 2: Discrete Jet  
(0.0691 events)

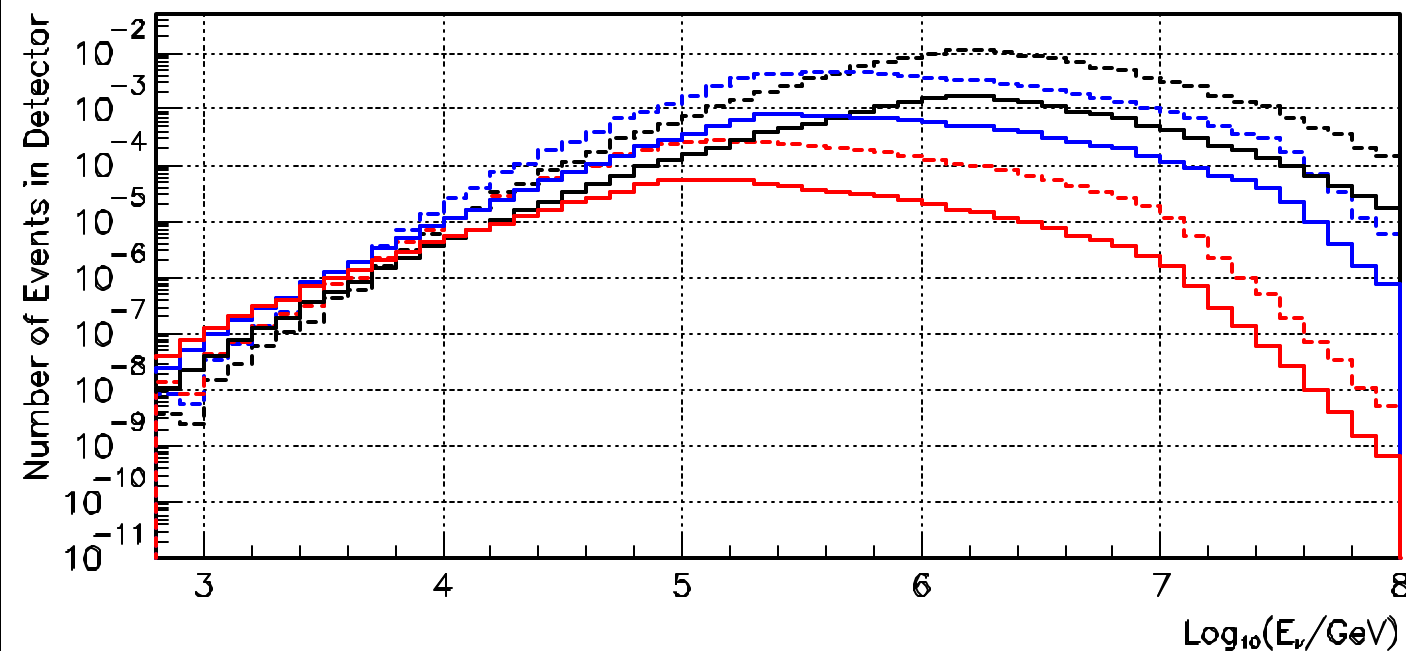
Model 3: Average Isotropic  
(0.0038 events)

### AMANDA-II (Solid)

Model 1: Discrete Isotropic  
(0.0202 events)

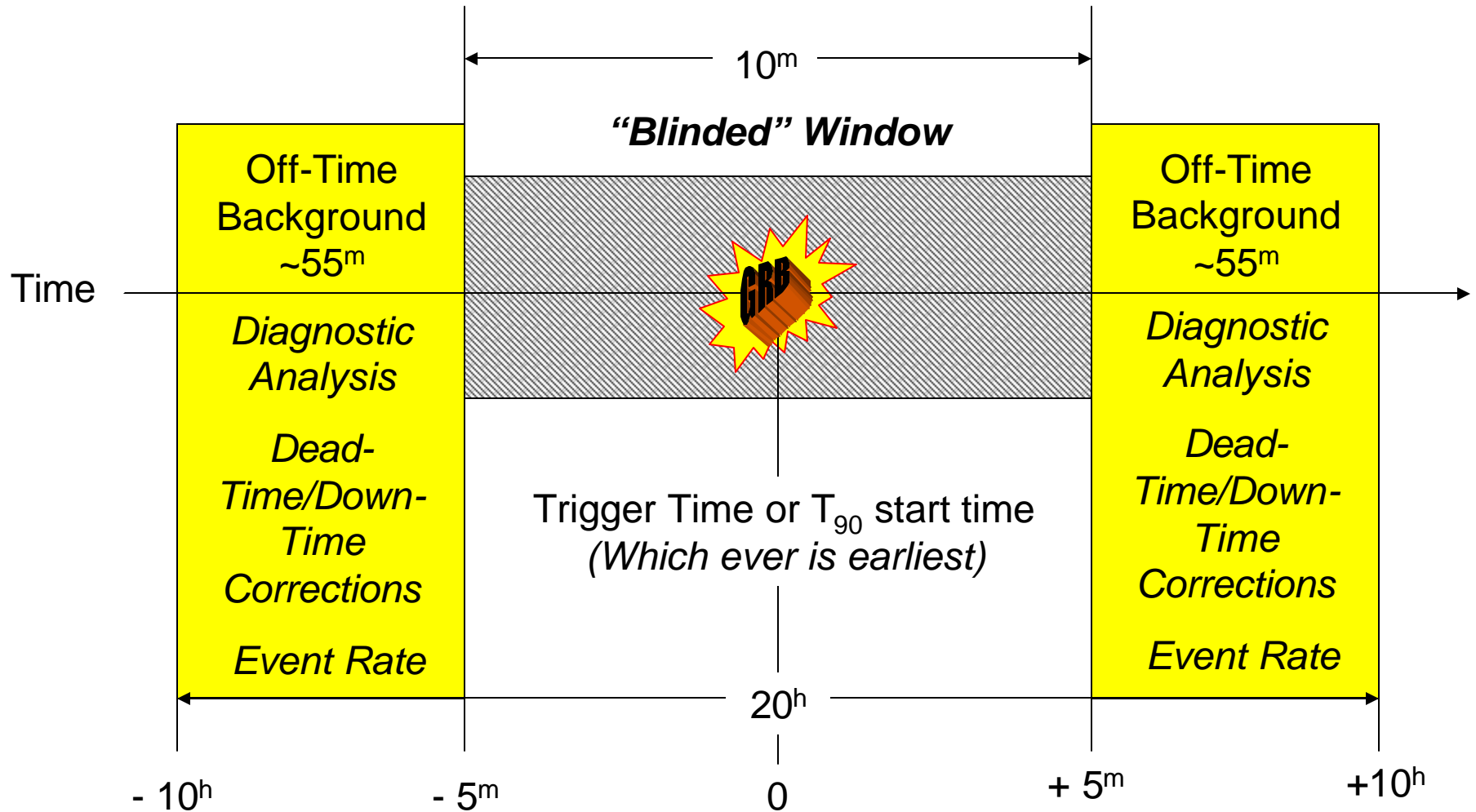
Model 2: Discrete Jet  
(0.0116 events)

Model 3: Average Isotropic  
(0.0008 events)



Order of magnitude differences in mean energy and number of events in detector.

# Statistical Blindness & Unbiased Analysis



Nominal Extraction:  $2^h$   
Nominal Off-Time Interval:  $110^m$



Systematic dead-time  
Down-time of detector



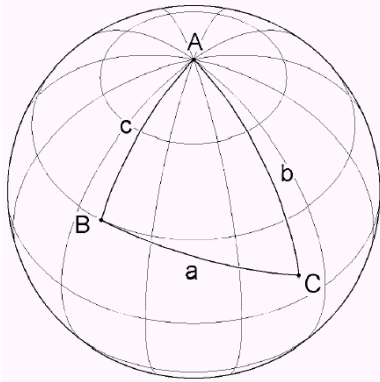
True Off-time  
Bkgd Event rate



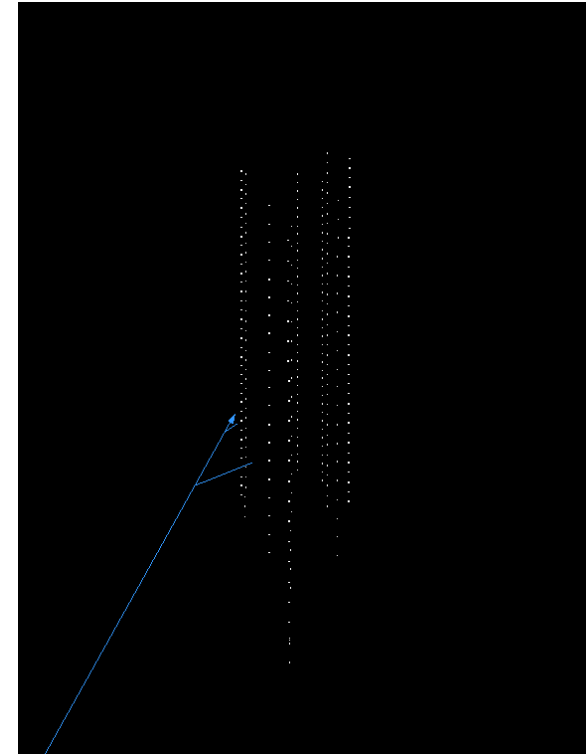
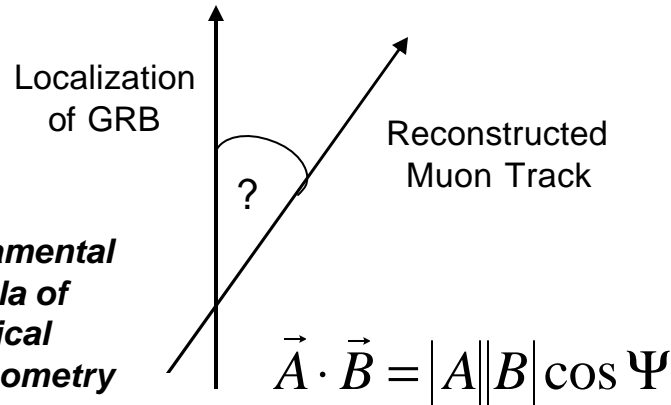
# Event Quality Selection: Optimization

- Multiple observables investigated → single, robust criterion emerged - maximum size of the search bin radius ( $\Psi$ ), i.e. the space angle between the reconstructed muon trajectory ( $\theta_\mu, f_\mu$ ) and the positional localization of the GRB ( $\theta_{\text{GRB}}, f_{\text{GRB}}$ ) :

$$\cos \Psi \equiv \sin \mathbf{q}_m \sin \mathbf{q}_{\text{GRB}} \cos(\mathbf{f}_m - \mathbf{f}_{\text{GRB}}) + \cos \mathbf{q}_m \cos \mathbf{q}_{\text{GRB}}$$

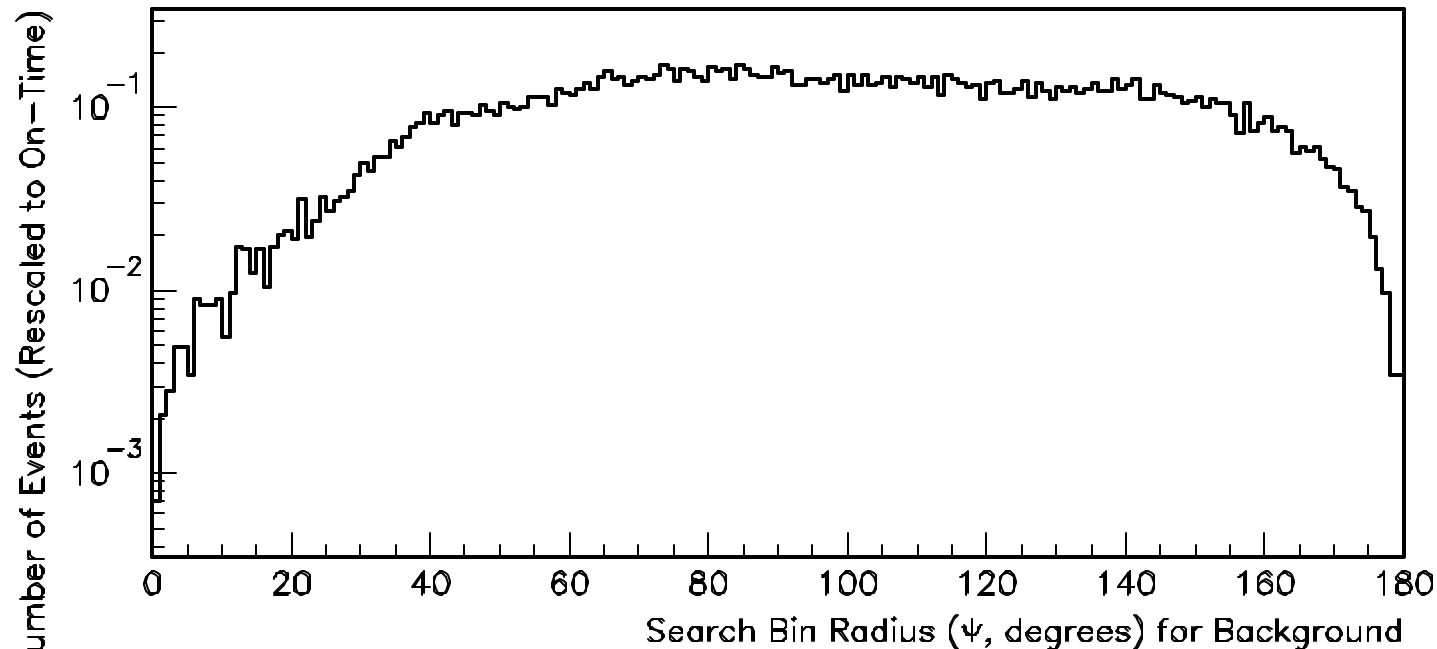


**Fundamental  
formula of  
spherical  
trigonometry**



- Up-going events topologically identified via maximum likelihood method.
- Method A: Best limit setting potential – Model Rejection Potential (MRP)  
Method → achieved via minimization of the model rejection factor (MRF):  $MRF \equiv \frac{n_{90}}{n_s}$   
*Hill & Rawlins Astropart. Phys. 19, 393-402 (2003), Feldman & Cousins Phys. Rev. D 57, 3873-3889 (1998)*
- Method B: Discovery potential – Model Discovery Potential (MDP)  
Method → achieved via minimization of the model discovery factor (MDF):  $MDF \equiv \frac{n'_{90}}{n_s}$   
*Hill, Hodges & Stamatikos (in preparation)*

On-Time Search Bin Radius Distribution for Background and Signal



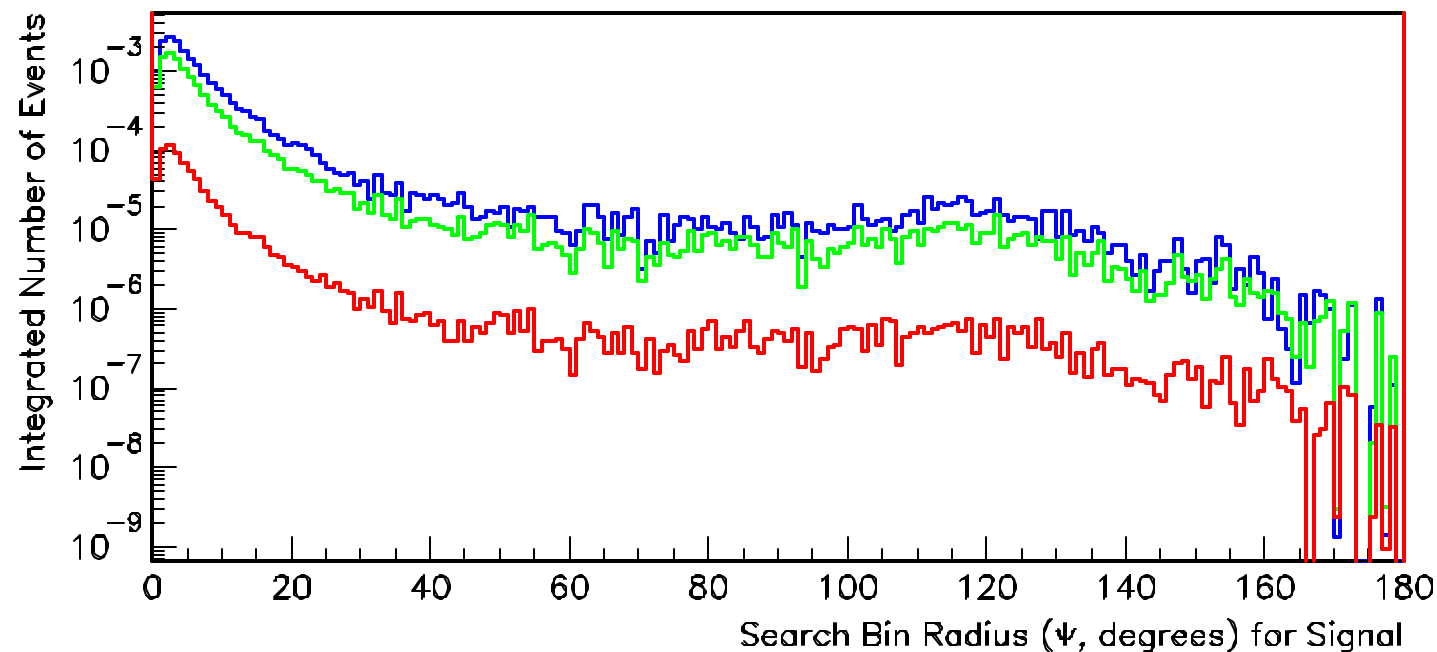
### Off-Time Background

$24,972 \pm 158$  Events in  
57,328.04 seconds.

Expected background  
rate:  $0.436 \pm 0.003$  Hz

Renormalized to  
search window  
duration  
(40/57,328.04).

$$n_b = 17.44 \pm 0.012$$



### On-Time Signal

Blue – Model 1

0.0202 Events

Green – Model 2

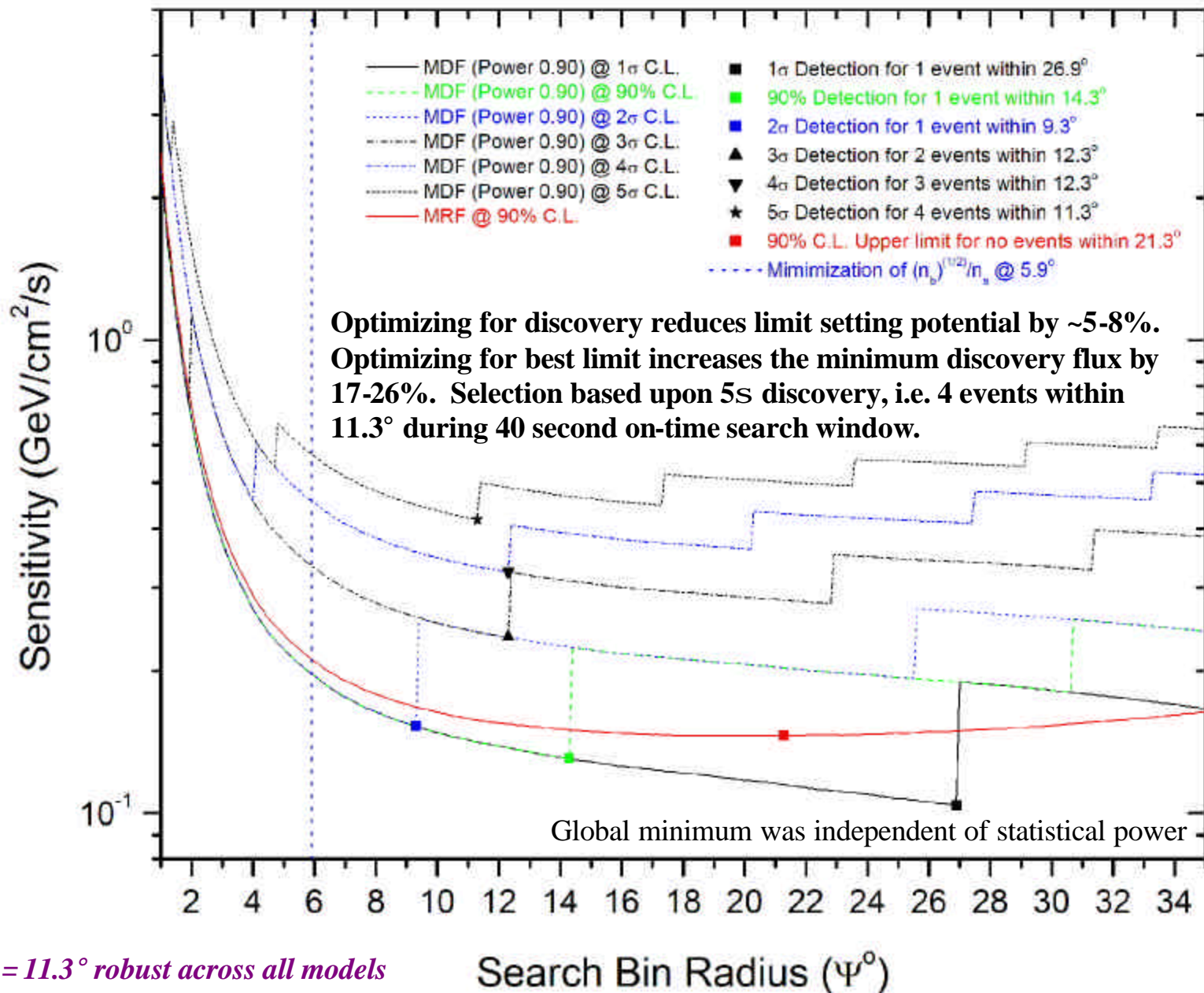
0.0116 Events

Red – Model 3

0.0008 Events

40 Seconds

### Signal Sensitivity as a Function of Search Bin Radius for Model 1

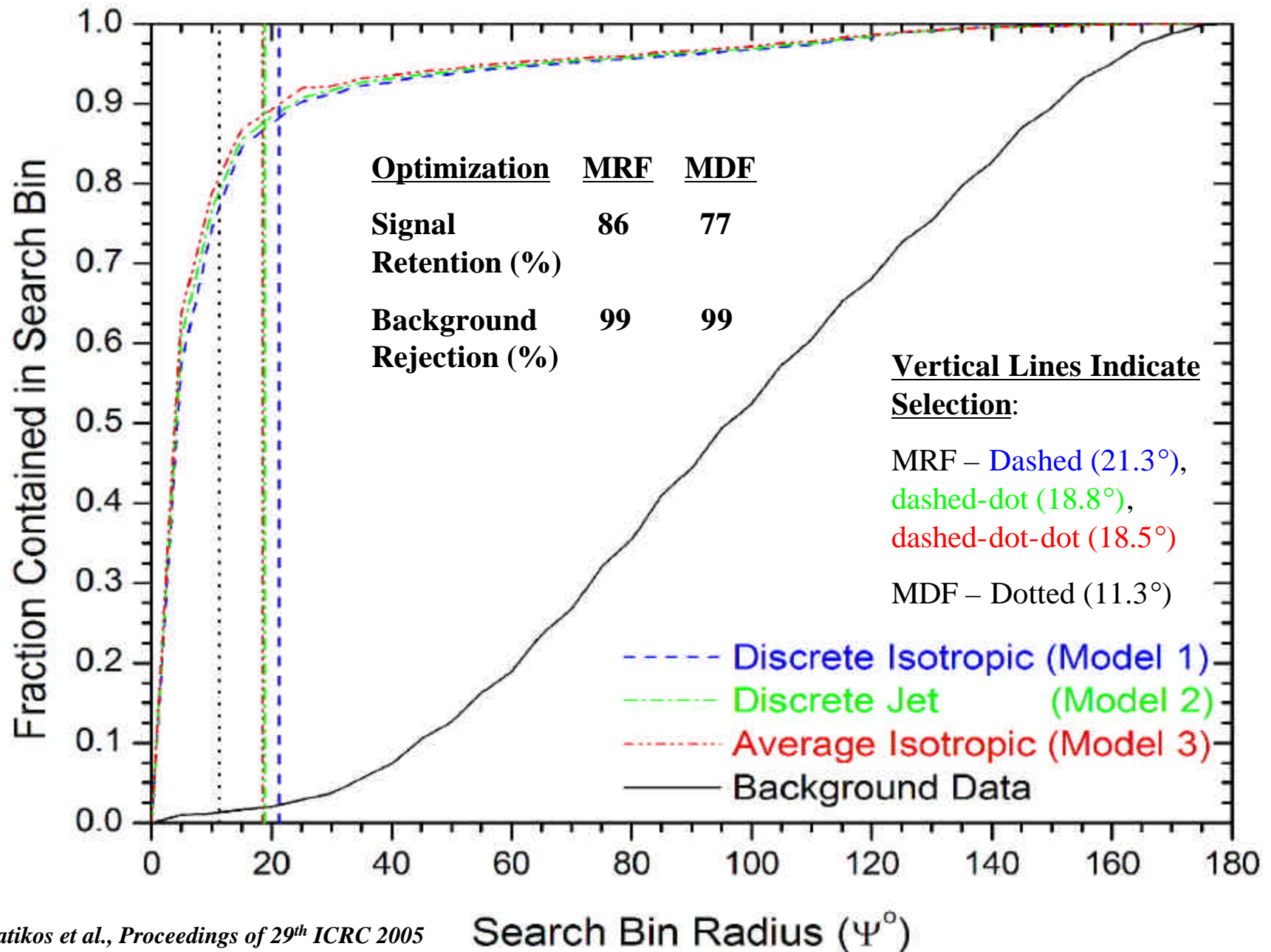


*$Y = 11.3^\circ$  robust across all models*

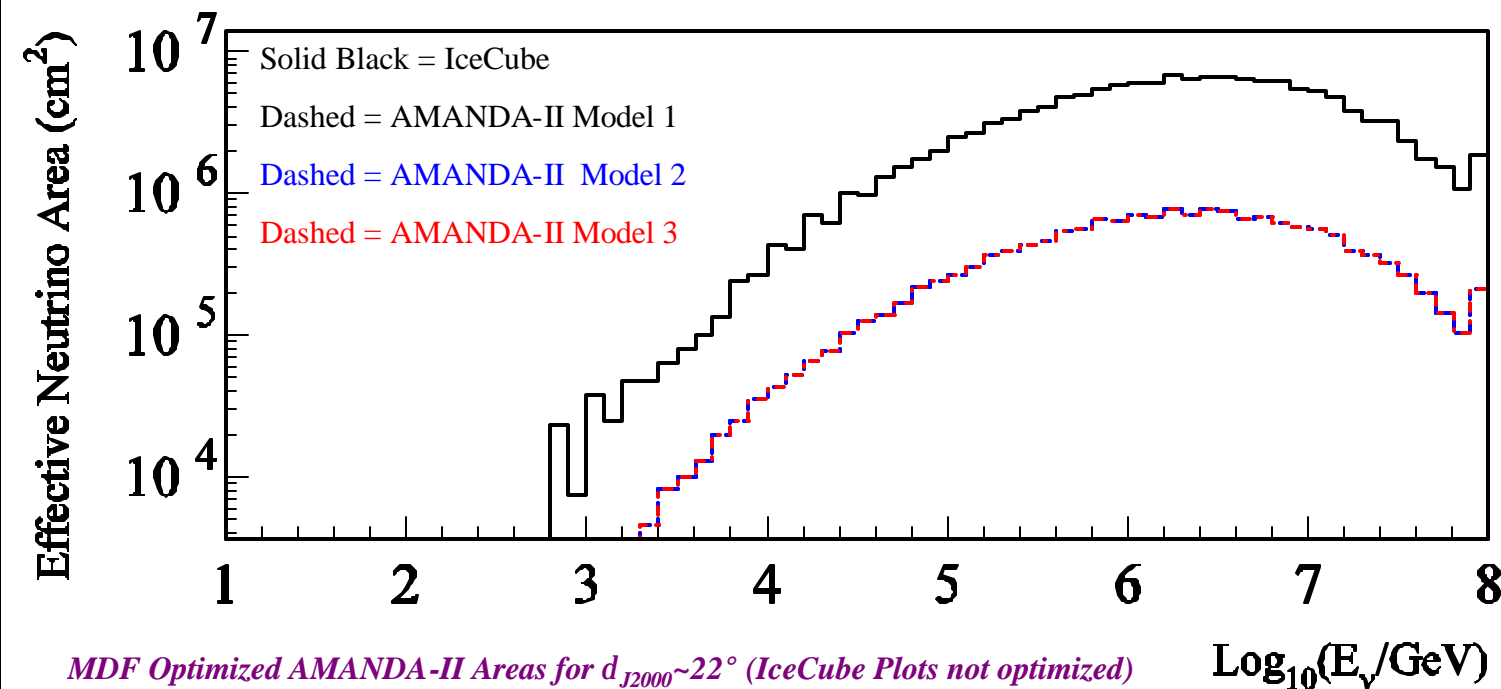
*MDF = Model Discovery Factor (Optimized for Detection)*

**MRF = Model Rejection Factor (Optimized for Best Upper Limit)**

# Signal Efficiency & Background Rejection







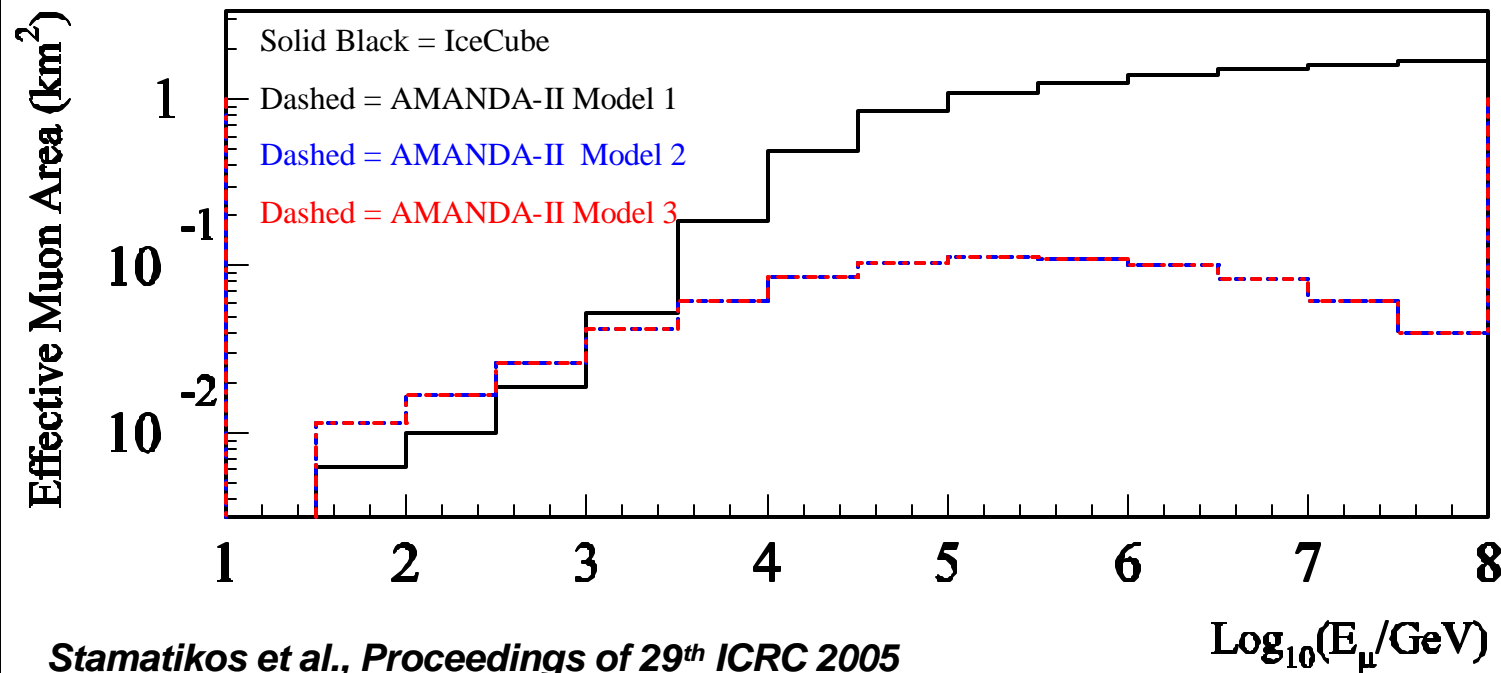
**Muon neutrino effective area:**

AMANDA-II:

$\sim 80 \text{ m}^2$  @  
 $\sim 2 \text{ PeV}$

IceCube:

$\sim 700 \text{ m}^2$  @  
 $\sim 2 \text{ PeV}$



**Muon effective area for energy at closest approach to the detector:**

AMANDA-II:

$\sim 100,000 \text{ m}^2$  @  
 $\sim 200 \text{ TeV}$

IceCube:

$\sim 1 \text{ km}^2$  @  
 $\sim 200 \text{ TeV}$

# Summary of Preliminary Results: GRB030329

Flux Model	Maximum Search Bin Radius		Expected Number of Background Events			Expected Number of Signal Events			Observed Number of Events		Optimization Method		GeV/cm <sup>2</sup> /s	
	Y <sup>A</sup> (°)	Y <sup>B</sup> (°)	n <sub>b</sub>	n <sub>b</sub> <sup>A'</sup>	n <sub>b</sub> <sup>B'</sup>	N <sub>s</sub>	n <sub>s</sub>	n <sub>s</sub> <sup>B'</sup>	n <sub>obs</sub>	n <sub>obs</sub> <sup>B</sup>	MRF (A)	MDF (B)	Sensitivity <sup>B</sup>	Limit <sup>B</sup>
1	21.3	11.3	17.44	0.23	0.06	0.1308	0.0202	0.0156	15	0	152	424	0.157	0.150
2	18.8	11.3	17.44	0.17	0.06	0.0691	0.0116	0.0092	15	0	256	716	0.041	0.039
3	18.5	11.3	17.44	0.17	0.06	0.0038	0.0008	0.0006	15	0	3864	10794	0.036	0.035

*Primed variables indicate value after selection. Superscripts indicate A=MRF and B=MDF optimization method.*

*Results consistent with null signal, and do constrain the models tested in AMANDA-II.*

## Comparison with Other Authors

1. The number of expected events in IceCube ( $N_s$ ) for model 1 is consistent with *Razzaque, Meszaros & Waxman Phys. Rev. D. 69 023001 (2004)*, when neutrino oscillations are considered.
2. The number of expected events in IceCube ( $N_s$ ) for model 3 is consistent with *Guetta et al, Astropart. Phys. 20, 429-455 (2004)*.
3. The number of expected events in IceCube ( $N_s$ ) for model 3 is consistent with *Ahrens et al., Astropart. Phys. 20, 507-532 (2004)* when the assumptions of *Waxman & Bahcall, Phys. Rev. D 59, 023002 (1999)* are considered.

# Conclusions & Future Outlook

1. Leptonic signatures from GRBs would be a smoking gun signal for hadronic acceleration; revealing a possible acceleration mechanism for high energy CRs as well as insight to the microphysics of the burst.
2. TeV-PeV neutrinos are observationally advantageous since correlative constraints lead to nearly background free searches.
3. Correlative leptonic observations of discrete GRBs should utilize the electromagnetic observables associated with each burst.
4. Although the event quality selection was robust across all models tested, observed variance in detector response unequivocally demonstrates the value of discrete modeling, especially in the context of astrophysical constraints on models for null results.
5. New era of sensitivity with Swift and IceCube – more complete electromagnetic descriptions of GRBs, e.g. redshift, beaming, etc. When not available, estimator methods exist for redshift and jet angle.
6. Similar results have been demonstrated in the context of a diffuse ensemble of GRBs [Becker, Stamatikos, Halzen, Rhode (submitted to Astroparticle Physics)].

# Synergy of Gamma-Ray & Neutrino Astronomy!



*Swift*  
2004



GLAS  
2007



AMANDA  
Since 1997



IceCube  
2005 - 2010